

Tropospheric ozone reduces carbon assimilation in trees: estimates from analysis of continuous flux measurements

SILVANO FARES*, RODRIGO VARGAS†, MATTEO DETTO‡, ALLEN H. GOLDSTEIN§, JOHN KARLIK¶, ELENA PAOLETTI|| and MARCELLO VITALE**

*Consiglio per la Ricerca e la sperimentazione in Agricoltura (CRA)- Research Centre for the Soil-Plant System, Via della Navicella 2-4, 00184 Rome, Italy, †Department of Plant and Soil Sciences, Delaware Environmental Institute, University of Delaware, Newark, DE 19716, USA, ‡Smithsonian Tropical Research Institute, MRC0580-06, Unit 9100 Box 0948, DPO, AA 34002-9998, USA, §Department of Environmental Science, Policy, and Management, University of California, Berkeley, 137 Mulford Hall, Berkeley, CA 94720, USA, ¶Cooperative Extension Kern County 1031 South Mount Vernon Avenue, Bakersfield, CA 93307, USA, ||National Research Council, Institute for Plant Protection, Via Madonna del Piano 10, Sesto Fiorentino (Florence) 50019, Italy, **Department of Environmental Biology, "Sapienza" University of Rome, Piazzale Aldo Moro 5, Rome 00185, Italy

Abstract

High ground-level ozone concentrations are typical of Mediterranean climates. Plant exposure to this oxidant is known to reduce carbon assimilation. Ozone damage has been traditionally measured through manipulative experiments that do not consider long-term exposure and propagate large uncertainty by up-scaling leaf-level observations to ecosystem-level interpretations. We analyzed long-term continuous measurements (>9 site-years at 30 min resolution) of environmental and eco-physiological parameters at three Mediterranean ecosystems: (i) forest site dominated by *Pinus ponderosa* in the Sierra Mountains in California, USA; (ii) forest site composed of a mixture of *Quercus* spp. and *P. pinea* in the Tyrrhenian sea coast near Rome, Italy; and (iii) orchard site of *Citrus sinensis* cultivated in the California Central Valley, USA. We hypothesized that higher levels of ozone concentration in the atmosphere result in a decrease in carbon assimilation by trees under field conditions. This hypothesis was tested using time series analysis such as wavelet coherence and spectral Granger causality, and complemented with multivariate linear and nonlinear statistical analyses. We found that reduction in carbon assimilation was more related to stomatal ozone deposition than to ozone concentration. The negative effects of ozone occurred within a day of exposure/uptake. Decoupling between carbon assimilation and stomatal aperture increased with the amount of ozone pollution. Up to 12–19% of the carbon assimilation reduction in *P. ponderosa* and in the *Citrus* plantation was explained by higher stomatal ozone deposition. In contrast, the Italian site did not show reductions in gross primary productivity either by ozone concentration or stomatal ozone deposition, mainly due to the lower ozone concentrations in the periurban site over the shorter period of investigation. These results highlight the importance of plant adaptation/sensitivity under field conditions, and the importance of continuous long-term measurements to explain ozone damage to real-world forests and calculate metrics for ozone-risk assessment.

Keywords: citrus, gross primary productivity, Mediterranean forest, ozone concentration, ozone damage, *Pinus ponderosa*, stomatal deposition

Received 22 January 2013 and accepted 12 March 2013

Introduction

Tropospheric ozone is a potent oxidizing agent and also a greenhouse gas, with background atmospheric concentrations in northern midlatitudes that have increased substantially in recent decades (Vingarzan, 2004; Cooper *et al.*, 2010). In Mediterranean regions, high solar radiation and temperatures promote photochemical reactions of anthropogenic and biogenic volatile organic compounds (VOC) and nitrogen oxides (NO_x), which

therefore produce ozone (Chameides *et al.*, 1988). Ozone can be removed from the atmosphere through plant stomatal uptake and deposition on soil, plant surfaces, or within the canopies after reacting with NO_x and biogenic VOC (Fowler *et al.*, 2009). Ozone has detrimental effects on living organisms, and the exposure to elevated ozone concentrations produces biochemical and physiological changes in plants. The main negative effect is the inhibition of carbon assimilation by damage of the photosynthetic apparatus in plants. Two meta-analysis reviews reported a reduction in light-saturated photosynthesis (–14%) and total tree biomass (–18%) of angiosperms in ozone treatments of around 40 ppb

Correspondence: Silvano Fares, tel. +39 06 7005413 127, fax +39 06 47836320, e-mail: silvano.fares@entecra.it

(Wittig *et al.*, 2007, 2009). Because of the difficulty of studying large and mature trees, however, these meta-analyses were based on young trees under controlled conditions with relatively low increases in ozone (e.g., <50 ppb). To quantify the effects on forests more generally, it is crucial to quantify the effects of low-to-high ambient ozone concentrations (e.g., from 10 to >80 ppb) on carbon assimilation and growth of mature and growing forests under field conditions (Manning, 2005).

In plant ecosystems, ozone has likely a negative effect on gross primary productivity (GPP), which represents the capacity of terrestrial ecosystems to capture CO₂ from the atmosphere. GPP is an important driver of the global carbon cycle, and >50% of total terrestrial GPP and net primary productivity (NPP; equivalent to GPP–autotrophic respiration) are accounted for by forests (Geider *et al.*, 2001; Grace, 2004). In consideration of the detrimental effect on vegetation, the international scientific community is working on establishing new criteria for protecting vegetation from ozone (Paoletti & Manning, 2007; UNECE, 2011). An overarching goal is to define a metric for ozone-risk assessment, which can identify at risk ecosystems to protect them using new standards and policies. In Europe and the USA, exposure-based indices have been widely used, under the assumption that plant injury and exposure to ozone concentrations are proportionally related (EPA, 2007; UNECE, 2011). Recently, a consensus is growing for moving toward a flux-based index (Matyssek *et al.*, 2007; Mills *et al.*, 2011). This index could be a measure to calculate the effective dose of ozone entering stomata, as this is recognized as the main deposition pathway responsible for plant damage (Matyssek *et al.*, 2007; UNECE, 2011). These issues demonstrate the

importance of quantifying and understanding potential ozone damage on carbon assimilation by plants at the ecosystem scale for policy-making and management decisions.

Traditional methods to assess ozone damage to vegetation and estimate metrics for ozone-risk assessment involve the use of plant chambers (e.g., cuvettes, open-top chambers). In these experimental setups, plants are exposed to known concentrations of ozone and controlled environmental conditions (Karlsson *et al.*, 2000; Manning, 2005). Although these approaches are useful to define standard conditions to calculate metrics, chambers make use of seedling or transplants, which may not have been adapted to long-term exposure to ozone, and may respond differently from adult trees; therefore, making it difficult to up-scale observations to ecosystem level (Samuelson & Kelly, 2001). Up-scaling these metrics to the ecosystem level is also challenging because: (i) the energy balance is not uniform within the canopy (Blanken *et al.*, 1997); (ii) ozone concentration decreases from canopy top to the soil, depending on the stomatal and nonstomatal ozone sinks, thus affecting in different extents different compartments of canopies (Wolfe *et al.*, 2011); and (iii) in Mediterranean regions, high values of vapor pressure deficit (VPD), temperature, and drought conditions can largely reduce stomatal conductance for long periods (Paoletti, 2006; Manes *et al.*, 2007). These limiting conditions challenge the application of stomatal deposition models, which predict stomatal conductance in response to environmental drivers (Emberson *et al.*, 2000; Fares *et al.*, 2013).

In this study, we used long-term datasets (>9 site-years) where biometeorological fluxes were directly measured at the ecosystem scale using the eddy covari-

Table 1 Monthly averages of air temperature (Ta), vapor pressure deficit (VPD), soil moisture, and ozone concentration ([O₃]) were recorded hourly and filtered for the day hours (9:00–19:00 hours). Precipitation (excluding irrigation), net ecosystem exchange (NEE), and ozone fluxes are reported as monthly sums. For Blodgett, errors refer to interannual averages. Negative sign means flux from the atmosphere to the canopies. na, not available

	Ta (°C)			VPD (kPa)			Precip. (mm)			Soil moisture (%)		
	Blodg.	Lind.	Cast.	Blodg.	Lind.	Cast.	Blodg.	Lind.	Cast.	Blodg.	Lind.	Cast.
Jan	6.64 ± 0.71	11.15	11.53	1.01 ± 0.05	0.34	0.30	110.73 ± 30.30	180.85	135.20	32.25 ± 1.05	20.13	16.91
Feb	6.69 ± 0.91	13.36	12.68	1.01 ± 0.06	0.40	0.56	185.43 ± 31.68	216.15	136.80	31.90 ± 1.04	20.72	19.37
Mar	9.80 ± 1.44	16.99	14.46	1.28 ± 0.11	1.06	0.54	180.82 ± 46.27	40.64	219.20	31.78 ± 0.99	17.67	22.85
Apr	9.66 ± 1.05	18.08	19.45	1.27 ± 0.09	1.11	0.97	155.66 ± 49.25	187.96	90.40	30.33 ± 1.51	20.14	16.70
May	16.87 ± 0.86	23.09	22.87	1.97 ± 0.10	1.95	1.17	67.84 ± 28.34	8.38	51.90	24.49 ± 1.66	20.68	11.63
Jun	20.96 ± 0.69	30.60	26.52	2.48 ± 0.09	3.27	1.28	17.42 ± 15.53	0.00	21.00	16.18 ± 1.63	16.16	9.33
Jul	24.65 ± 0.45	33.42	27.32	3.03 ± 0.09	3.73	1.46	7.85 ± 7.85	0.00	51.00	10.72 ± 0.94	21.76	8.53
Aug	24.48 ± 0.32	31.66	29.87	2.98 ± 0.05	3.43	2.05	35.84 ± 35.39	0.00	2.00	9.32 ± 0.60	25.29	8.52
Sep	21.12 ± 0.75	29.04	27.36	2.49 ± 0.10	2.77	1.58	13.27 ± 4.93	2.54	45.00	9.48 ± 0.32	29.08	8.30
Oct	15.53 ± 0.89	21.73	19.96	1.80 ± 0.10	1.33	1.03	48.79 ± 26.95	173.82	347.60	11.46 ± 1.23	25.87	8.14
Nov	9.14 ± 0.77	15.83	15.18	1.19 ± 0.06	0.79	0.58	163.03 ± 36.52	40.64	180.50	23.62 ± 1.06	17.91	8.66
Dec	5.77 ± 0.63	10.19	12.15	0.94 ± 0.04	0.32	0.46	267.94 ± 50.20	128.52	295.50	30.96 ± 1.02	20.38	10.70

ance technique (Fares *et al.*, 2010a). The main objective of this study was to explore the interactions between atmospheric ozone concentration and stomatal deposition to ozone with GPP, to quantify potential damage to vegetation in Mediterranean climates. We hypothesize that high levels of ozone concentration (e.g., >75 ppb) in the atmosphere and/or stomatal fluxes result in a decrease in carbon assimilation by trees under field conditions. Furthermore, we used novel techniques for time series analysis (i.e., wavelet coherence analysis and Granger causality), and general regression models to determine whether ozone concentration and/or stomatal ozone deposition can be used as predictors of ozone damage on GPP. The experiments were performed at three field sites all located in geographical areas characterized by Mediterranean climates and exposed to phytotoxic levels of ozone produced by photochemical processing of emissions from nearby urban centers.

Material and methods

Description of sites

The Blodgett Ameriflux site (38°53'42.9"N, 120°37'57.9"W) is located at 1315 m a.s.l. in the Sierra Nevada Mountains of California, near Georgetown, adjacent to the UC Berkeley Blodgett Forest Research Station, on land owned by Sierra Pacific Industries in the United States of America (USA). This forest site is a plantation of Ponderosa pine (*Pinus ponderosa* L.) planted in 1990. The major understory shrubs are Manzanita (*Arctostaphylos manzanita*) and Ceanothus (*Ceanothus cordulatus*). The total Leaf Area Index (LAI) increased from 1.2 in 2001 to 2.9 m²_{leaf} m⁻²_{ground} in 2006, with a mean height increasing from 4 m to 7.6 m during the same period (details

on forest silvicultural practices and soil conditions are given in Goldstein *et al.*, 2000; Fares *et al.*, 2010a). The site is characterized by a Mediterranean climate, with warm dry summers (mean monthly air temperature >20 °C, and mean summer precipitation <150 mm; Table 1), and cold wet winters (mean monthly temperature ca. 6 °C, and mean winter precipitation >700 mm; Table 1). There is a typical mountain wind regime bringing daytime air up the mountain slopes from the nearby Sacramento valley urban area, whereas at night, a gentle downslope wind reverses the direction. The soil has 60% sand and 29% loam with a pH of 5.5. More details on forest climate conditions are given in Fares *et al.* (2010a).

The Lindcove measurement site is located in a private Valencia Orange orchard with *Citrus sinensis* planted in the 1960s, 131 m a.s.l., 3 km west of the University of California Lindcove Research and Extension Centre near Visalia, California, USA (36°21'23.6"N, 119°5'32.1"W). The site is characterized by a Mediterranean climate, with warm dry summers (mean monthly air temperature >30 °C, and mean summer precipitation <150 mm; Table 1), and cold wet winters (mean monthly air temperature <9 °C, and mean winter precipitation >700 mm; Table 1). The site has a typical wind pattern, which brings daytime air up the mountain slopes of the Sierra Nevada Mountains from the nearby urban area of Visalia, whereas at night, a gentle downslope wind reverses the direction. The soil texture is 42% sand, 38% silt, and 20% clay. The plantation is well irrigated, and for a more detailed description on soil and plant characteristics, spacing of the plantation, irrigation treatments, and climate characteristics, see Fares *et al.* (2012).

The experimental site of Castelporziano (41°44'41.9"N, 12°24'32.9"E) is located 80 m a.s.l. and 7 km from the seashore of the Tyrrhenian Sea inside the Presidential Estate of Castelporziano, an area of about 6000 ha located 25 km SW from the center of Rome, Italy. This Thermo-Mediterranean region is characterized by prolonged stress aridity during summer periods, and a moderate cold stress during winter. The wind circulation is mostly determined by a local sea-land

NEE (g C m ⁻²)			[O ₃] (ppb)			O ₃ flux (g O ₃ m ⁻²)			St. O ₃ flux (g O ₃ m ⁻²)		
Blodg.	Lind.	Cast.	Blodg.	Lind.	Cast.	Blodg.	Lind.	Cast.	Blodg.	Lind.	Cast.
-11.93 ± 12.94	-37.78	na	33.98 ± 1.99	20.12	na	-0.31 ± 0.02	-0.30	na	-0.06 ± 0.01	na	na
-42.33 ± 14.17	-5.71	na	37.97 ± 2.40	26.73	na	-0.33 ± 0.02	-0.52	na	-0.11 ± 0.01	na	na
-111.88 ± 23.83	-38.50	na	43.27 ± 2.40	41.16	na	-0.44 ± 0.02	-0.60	na	-0.14 ± 0.01	na	na
-188.30 ± 26.27	25.51	na	45.99 ± 2.45	45.71	na	-0.59 ± 0.03	-0.62	na	-0.19 ± 0.01	-0.03	na
-263.35 ± 38.07	-42.64	na	52.53 ± 2.18	50.94	na	-0.88 ± 0.04	-0.67	na	-0.19 ± 0.02	-0.12	na
-271.37 ± 33.35	3.23	na	54.84 ± 2.65	61.19	na	-0.93 ± 0.04	-0.65	na	-0.15 ± 0.01	-0.12	na
-282.95 ± 39.66	89.01	na	59.05 ± 3.66	72.21	na	-0.98 ± 0.04	-0.80	na	-0.11 ± 0.01	-0.16	na
-230.39 ± 41.92	36.75	na	63.92 ± 3.24	66.39	na	-0.84 ± 0.04	-0.78	na	-0.10 ± 0.01	-0.16	na
-146.81 ± 42.09	-37.11	101.01	55.77 ± 2.86	64.40	46.72	-0.52 ± 0.03	-0.72	-0.07	-0.09 ± 0.01	-0.17	-0.03
-77.07 ± 22.07	-6.28	123.82	45.61 ± 4.00	41.11	34.76	-0.46 ± 0.02	-0.65	-0.24	-0.08 ± 0.01	-0.21	-0.11
-9.69 ± 11.07	-57.72	159.93	33.95 ± 2.25	28.59	17.20	-0.40 ± 0.02	-0.53	-0.10	-0.07 ± 0.01	-0.10	-0.09
21.84 ± 12.76	-39.08	48.75	31.74 ± 1.82	20.52	23.54	-0.33 ± 0.02	-0.43	-0.06	-0.09 ± 0.04	na	-0.03

breeze wind regime, with moderate-to-strong S–SW winds blowing during the morning, and light N–NE winds in the afternoon. The soil has a sandy texture (sand content above 60%) and low water-holding capacity, which exacerbates early drought. The vegetation is a mixed Mediterranean forest with shrub and tree species with an average height of 25 m and a LAI of $4.76 \text{ m}^2_{\text{leaf}} \text{ m}^{-2}_{\text{ground}}$. The main tree species are as follows: *Arbutus unedo*, *Laurus nobilis*, *Phyllirea latifolia*, *P. pinea*, *Quercus ilex*, and *Q. suber*. These species belong to an uneven-aged stand where the oldest trees were planted more than 80 years ago. More details on soil properties and site characteristics are provided in Fares *et al.* (2013).

Gas exchange measurements

Measurements used in this study from the Blodgett forest started in January 2001 and ended in December 2007 (7 site-years). Measurements in Lindcove started in October 2009 and ended in November 2010 (>1 site-year), and measurements in Castelporziano started in September 2011 and ended in December 2011 (<1 site-year). At all sites, soil moisture, air temperature, relative humidity, photosynthetically active radiation, and atmospheric pressure were measured continuously at 30 min time intervals. Concentration measurement of water, CO_2 , and ozone was performed continuously and at high frequency (10 Hz) and correlated with the vertical wind velocity measured with an ultrasonic anemometer to calculate fluxes according to the eddy covariance technique extensively described elsewhere (Goldstein *et al.*, 2000; Detto *et al.*, 2010). Details on instrumentation used to measure fluxes, corrections, and uncertainty analysis are provided in Fares *et al.* (2010b) for the Blodgett site, in Fares *et al.* (2012) for Lindcove, and Fares *et al.* (2013) for Castelporziano. GPP was calculated from ecosystem scale fluxes of CO_2 directly measured by eddy covariance Net Ecosystem Exchange (NEE) by adding the ecosystem respiration term (R_{eco}) to NEE. R_{eco} was calculated using the nighttime NEE measurements and extrapolated to the daytime according to the model formulation explained in detail by Lasslop *et al.* (2010).

In this study, we indicate negative fluxes when mass and energy transfer are from the atmosphere into the vegetation and soil. To calculate a canopy-scale stomatal conductance to ozone (G_{O_3}), we used measurements of latent heat flux evapotranspiration (ET) according to the Evaporative-Resistance method, commonly used in multiple studies. Details of the calculation (Eqn S1) and additional references for this technique are shown in the supplementary material.

Statistical analyses

Wavelet coherence analysis. We used wavelet analysis as a time series technique that has been widely applied in the geosciences (Torrence & Compo, 1998) and has recently been applied for studying ecosystem biometeorological variables (Vargas *et al.*, 2010, 2011; Heinemeyer *et al.*, 2012). This technique is used to quantify the spectral characteristics of time series that may be nonstationary and heteroscedastic. Analyses using Fourier transform or cross-correlation to investigate the spectral properties of biometeorological variables failed in

the presence of nonstationary phenomena (Katul *et al.*, 2001), such as rain pulses, heat waves, or freezing events. Most biometeorological variables (e.g., GPP, G_{O_3}) typically violate the stationarity assumption underlying the analysis of spectral properties and wavelet analysis is an alternative technique to analyze them (Torrence & Compo, 1998). In this study, we explored the temporal correlation between GPP with ozone concentrations (hereon indicated with $[\text{O}_3]$) and G_{O_3} using wavelet coherence analysis (Grinsted *et al.*, 2004). Previous reports have described the technique in detail for climate studies (Torrence & Compo, 1998; Grinsted *et al.*, 2004) and soil CO_2 efflux research (Vargas *et al.*, 2010). Briefly, coherency is roughly similar to classical correlation, but it pertains to the oscillating components in a given time period (e.g., 1 day period or 8 day period).

It is important to recognize that the diurnal cycle of solar radiation governs the daily course of air temperature, GPP, and ozone photochemical production contributing to confounding effects (Vargas *et al.*, 2011; Heinemeyer *et al.*, 2012). Therefore, changes in light and air temperature could mask or overestimate the temporal correlation between GPP and $[\text{O}_3]$ or G_{O_3} . Thus, to analyze these temporal correlations, we removed the effect of photosynthetic active radiation (PAR) and air temperature (Ta) on GPP, G_{O_3} , and $[\text{O}_3]$. In other words, we used the residuals of these time series, which could be interpreted as the light and temperature independent time series of these variables. This is a conservative approach to analyze temporal correlations when confounding effects are suspected (Vargas *et al.*, 2011; Heinemeyer *et al.*, 2012). To do this, we first removed the effect of changes in PAR on all variables by fitting independent simple linear regressions for each day calculated from hourly measurements with the form:

$$\text{Residuals}_1 = \text{Var}_x - (B_1 + B_2 * \text{PAR}) \quad (1)$$

where B_1 and B_2 are parameters evaluated for each single day based on half hourly measurements of PAR and Var_x is the biometeorological variable of interest (e.g., GPP). Thus, in this first step, the biometeorological variable of interest was detrended for daily changes in PAR. Second, we fit a second set of simple linear regressions for each day on the Residuals_1 newly created time series with the form:

$$\text{Residuals}_2 = \text{Residuals}_1 - (B_3 + B_4 * \text{Ta}) \quad (2)$$

where B_3 and B_4 are parameters evaluated for each single day based on half hourly measurements of Ta. Thus, the result of Residuals_2 is that the biometeorological variable of interest was detrended for daily changes in PAR and Ta. Using this conservative approach, we propose that any temporal correlation between the residuals of daily GPP and G_{O_3} or $[\text{O}_3]$ is likely to represent a link without the influence of confounding effects. All analyses were performed using MATLAB R2007a (The MathWorks Inc., Natick, MA, USA).

General regression model. The General Regression Model (GRM) applies the methods of the general linear model, allowing it to build models for designs with multiple-degrees-of-freedom effects for categorical predictor variables, as well as for designs with single-degree-of-freedom effects for continuous predictor variables. The GRM approach used here

implements stepwise and best-subset model-building techniques for Analysis of Variance (ANOVA), regression, and analysis of covariance (ANCOVA) designs. To build models and to estimate and test hypotheses about effects included in the final model, the least squares method of the general linear model was applied. The regression equation for a linear regression design for three continuous predictor variables P , Q , and R is as follows:

$$Y = b_0 + b_1P + b_2Q + b_3R \quad (3)$$

The predictors among four case studies here investigated were as follows: PAR ($\mu\text{mol m}^{-2}\text{s}^{-1}$), air temperature (T_a , $^{\circ}\text{C}$), vapor pressure deficit (VPD, kPa), soil moisture (%), canopy transpiration (ET, $\text{mmol m}^{-2}\text{s}^{-1}$), and stomatal ozone deposition (G_{O_3} , m s^{-1}). Data averaged for 30 min time resolution were used in the model. The model was designed with 70% of the dataset and then cross-validated with the remaining 30% of the data.

In addition to linear regression analysis, we performed a nonlinear regression approach that includes polynomial regression designs to degree 2 and additionally the two-way interaction (i.e., combination) effects of the predictor variables (Eqn S2).

Random Forest Analysis (RFA). Random Forest module is a complete implementation of the random forest (RF) algorithm (Breiman *et al.*, 1984; Breiman, 2001). This technique can be used for regression-type problems (to predict a continuous dependent variable) as well as classification problems (to predict a categorical dependent variable). A RF consists of a collection (i.e., ensemble) of simple tree predictors, each capable of producing a response when presented with a set of predictor values. During the building of each tree, for each split – that is for each node – predictor statistics (i.e., sums of squares regression, as simple regression trees are built in all cases) are computed for each predictor variable; the best predictor variable will then be chosen for the actual split. The final predictor importance values are computed by normalizing those averages, so that the highest average is assigned the value of 1, and the importance of all other predictors is expressed in terms of the relative magnitudes of the average values of the predictor statistics, relative to the most important predictor. For this analysis, we used the same predictors at the same time resolution used for the GRM analysis. A more detailed description of this method is provided in the supplementary material. All analyses were done with STATISTICA 8.0 (StatSoft Inc., Tulsa, OK, USA).

Granger causality. G-causality explains phenomena by showing them to be a result of effects originating from prior causes in time as a signal processing technique. When these prior causes are accounted for, predictions of the phenomenon are improved against a null hypothesis that does not account for these prior causes. This is the statistical interpretation of causality proposed by Granger (1969) and is commonly referred to as Granger or G-causality. This causality metric originated in econometrics, but is now proliferating to a number of disciplines including ecology (Detto *et al.*, 2012).

G-causality is a measure of coupling with time and directionality. For this reason, it is based on prediction errors rather than on linear interactions among coefficients. Traditionally, it is expressed as the ratio between the residual variance of the bivariate and univariate autoregressive models, σ_{η}^2 and σ_{ϵ}^2 respectively, and is given as:

$$G_{Y \rightarrow X} = \ln \frac{\sigma_{\eta}^2}{\sigma_{\epsilon}^2}. \quad (4)$$

If the variables X and Y do not interact, there will be no improvement in using Y to predict X , i.e., $\sigma_{\epsilon}^2 \approx \sigma_{\eta}^2$ and $G_{Y \rightarrow X} \approx 0$, even if the two variables are correlated. If otherwise Y has a causal influence on X , $\sigma_{\epsilon}^2 < \sigma_{\eta}^2$ so $G_{Y \rightarrow X} > 0$.

G-causality can be formulated in the spectral domain and extended to multivariate systems. A more detailed explanation of this technique is provided in the supplementary material.

Results

Study of temporal correlations using wavelet coherence analysis

This analysis was performed to study the temporal correlations between the residuals of GPP and $[O_3]$ or G_{O_3} at all study sites. For the Blodgett forest, we found a strong temporal correlation (denoted by the red colors) between the residuals of GPP and atmospheric $[O_3]$ (Fig. 1a), and between GPP and G_{O_3} at the 1 day period (Fig. 1b). This temporal correlation at the 1 day period was in phase (zero lags), and was not constant throughout the years as it was present only for 18.3% of the measured days (denoted by the red colors, Fig. 1c and S1). Higher temporal correlation was associated with low values of GPP (Fig. 1e), and higher $[O_3]$ (Fig. 1f) as denoted by black broken lines in two examples in Fig. 1. Seasonal variations also showed significant temporal correlations, with 15% of the days, which showed temporal correlation between GPP and $[O_3]$ at the 64 day period.

For the Lindcove site, we also found a strong temporal correlation between the residuals of GPP and $[O_3]$ (Fig. 2a) or G_{O_3} (Fig. 2b) mainly at the 1 day period (48% of the measured days denoted by the red colors in Fig. 2c), but it was also not consistent throughout the measured year. The wavelet analysis (data not shown) indicated a temporal correlation at the 1 day period of 2 h lag (i.e., G_{O_3} rises before GPP). Although this research site has only 1 year of measurements, higher temporal correlations (red colors in Fig. 2c and d) were also present at lower values of GPP (Fig. 2e) and higher $[O_3]$ (Fig. 2f), as denoted by the broken lines in Fig. 2.

Also for the Castelporziano site, we found a strong temporal correlation between the residuals of GPP and $[O_3]$ (Fig. 3a) or G_{O_3} (Fig. 3b) mainly at the 1 day period (40% of the measured days denoted by the red

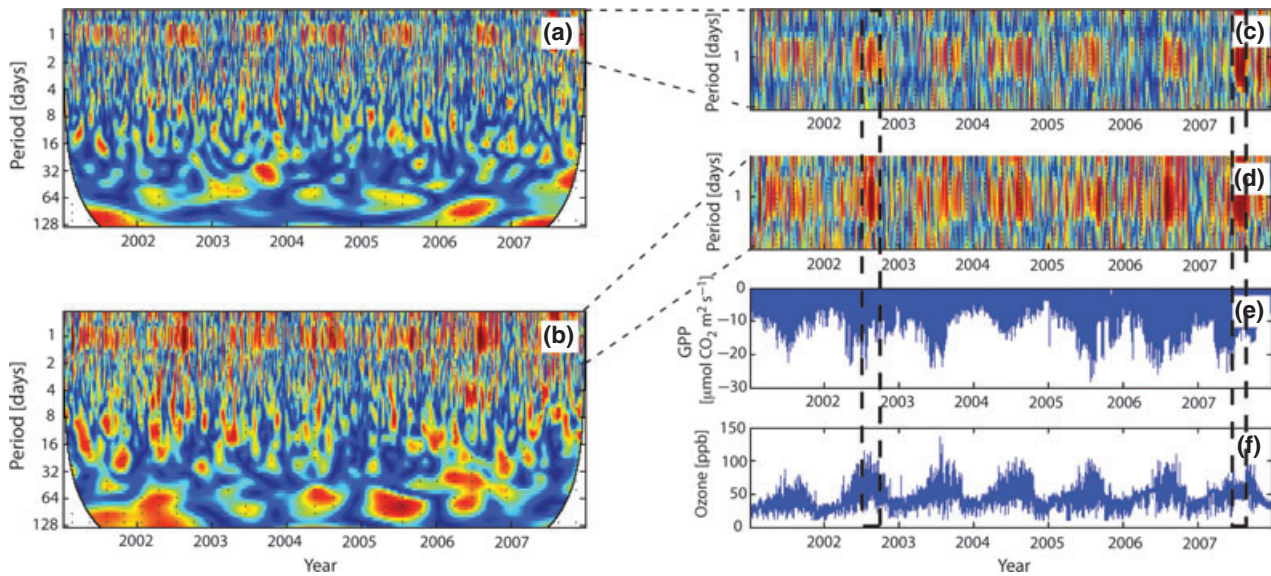


Fig. 1 Wavelet coherence analysis to look the temporal correlations between the residuals of gross primary productivity (GPP) and ozone concentration (a, c) or stomatal ozone deposition (b, d) for the Blodgett site. The colors for power values are from blue (low temporal correlations with GPP) to red (high temporal correlations with GPP). The thick black line in a and b indicates the cone of influence that delimits the region not influenced by edge effects. Black broken boxes show examples of strong correlation (denoted by red colour in c, d) between low GPP values and high ozone concentrations. See Fig. S1 for details on temporal correlations at the 1 day time period.

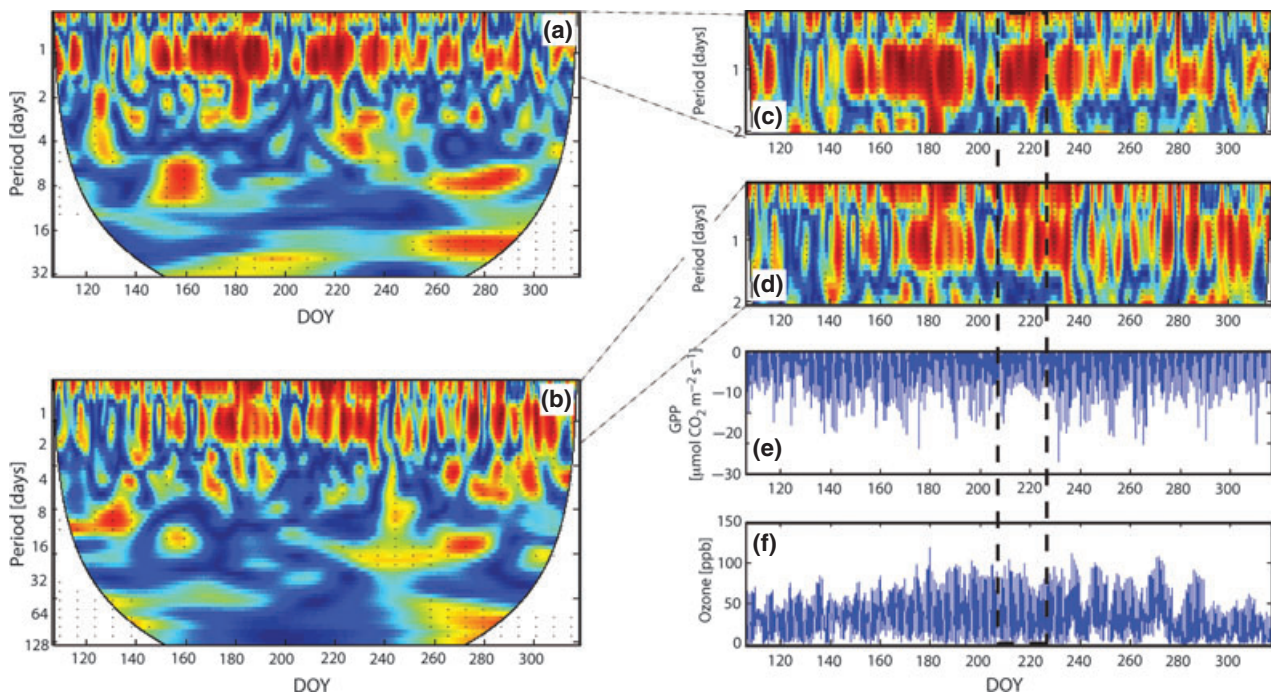


Fig. 2 Wavelet coherence analysis to look the temporal correlations between the residuals of gross primary productivity (GPP) and ozone concentration (a, c) or stomatal ozone deposition (b, d) for the Lindcove site. The colors for power values are from blue (low temporal correlations with GPP) to red (high temporal correlations with GPP). The thick black line in a and b indicates the cone of influence that delimits the region not influenced by edge effects. Black broken boxes show examples of strong correlation (denoted by red color in c, d) between low GPP values and high ozone concentrations. Days of the year (DOY), days after January 20th of year 2010.

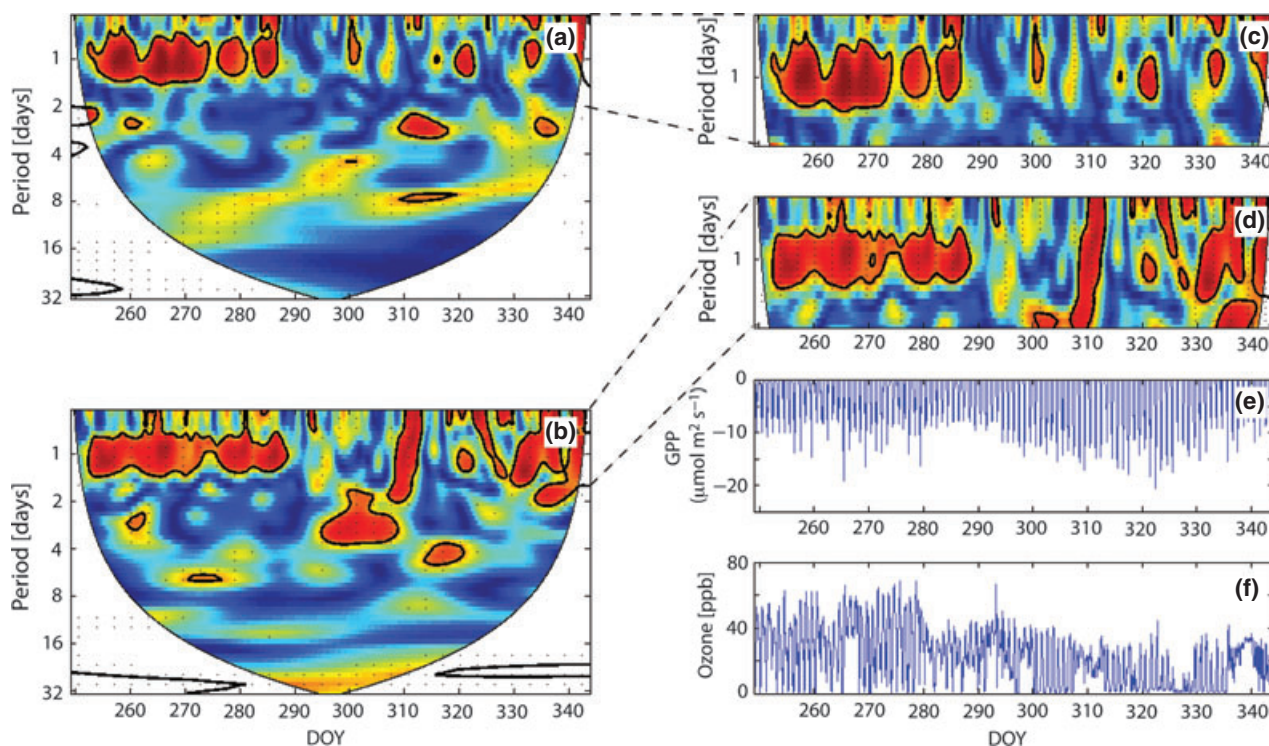


Fig. 3 Wavelet coherence analysis to look the temporal correlations between the residuals of gross primary productivity (GPP) and ozone concentration (a, c) or stomatal ozone deposition (b, d) for the Castelporziano site. The colors for power values are from blue (low temporal correlations with GPP) to red (high temporal correlations with GPP). The thick black line in a and b indicates the cone of influence that delimits the region not influenced by edge effects. Days of the year (DOY), days after September 1st of year 2011.

colors in Fig. 3c and d), but constant only in the warm seasons [Days of the year (DOY) 244–289]. The temporal correlation at the 1 day period was in phase (zero lags). Higher temporal correlations (red colors in Fig. 3c and d) were also present at lower values of GPP (Fig. 3e) and higher $[O_3]$ (Fig. 3f).

The following step was to evaluate our hypothesis to test whether increasing ozone concentrations change the relationship between GPP and G_{O_3} . In all study sites, the strongest temporal correlation was at the 1 day period; therefore, we extracted the information from each time series from this time period. In other words, we removed the information for other time periods (i.e., frequencies larger than 1 day) to analyze the relationship between G_{O_3} and GPP. Our analysis was based on the residuals of GPP and the residuals of G_{O_3} (i.e., to avoid confounding effects) and grouped by three ranges of atmospheric ozone concentrations: low (<50 ppb), medium (>50 and <75 ppb), and high (>75 ppb). At both Blodgett and Lindcove sites, we found that when G_{O_3} increased, GPP also increased as both fluxes are related to stomata opening. However, the slope of this relationship decreased from 0.24 to 0.11 and from 0.20 to 0.12 as atmospheric ozone concentration increased from low to high ozone for Blodgett and Lindcove,

respectively (Fig. 4). The large dataset for Blodgett allowed calculating the slopes for each year of these relationships. We found large interannual variability in the value of the slopes between different ozone concentrations; especially for years 2004 and 2006 (Fig. S2; Table S1). In Castelporziano, GPP greatly increased as G_{O_3} increased at low ozone concentrations, but responses to higher levels of ozone concentration were not studied as ozone rarely exceeded 50 ppb at this site.

Statistical models to highlight dependence of GPP on ozone

Four case studies were selected in both linear and non-linear models. Case 1 included the environmental variables, which are known to control GPP (i.e., PAR, T_a , and soil moisture). The signs of the coefficients of predictors in the linear model are negative for variables maximizing carbon assimilation, and positive for those that represent a constraint (Table 2). For the nonlinear model (Table S1), the behavior of predictors and their combination was more complicated in relation to their relationships with GPP (Table S2). Due to nonlinear nature of these relationships, signs of predictors could change in relation to a given combination of predictors.

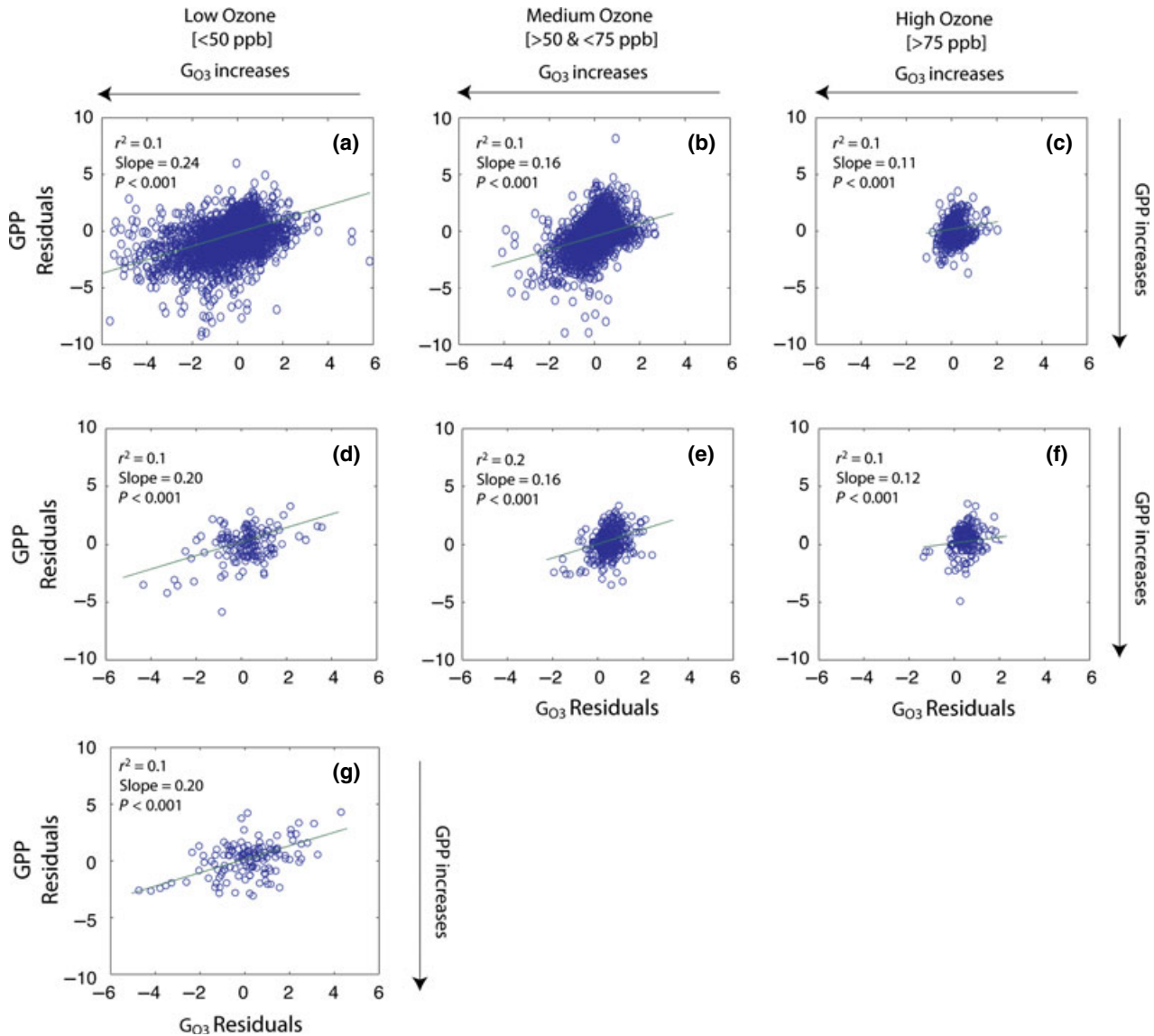


Fig. 4 Relationship between the residuals of gross primary productivity (GPP) at the 1 day time period and the residuals of stomatal ozone deposition (G_{O_3}) at the 1 day time period for grouped episodes of atmospheric ground-level ozone concentration: low (<50 ppb), medium (>50 and <75 ppb), and high (>75 ppb). Charts a, b, c refer to Blodgett forest, charts d, e, f refer to Lindcove, and chart g to Castelporziano (note that ozone concentrations rarely exceeded 50 ppb at this site).

In Blodgett and Lindcove, PAR is the predictor that better explained GPP (Table 2), followed by VPD, T_a , and soil moisture. In Castelporziano, a more drought-stressed ecosystem, soil moisture is the predictor statistically more relevant, which was also lower in comparison with the other ecosystems (Table 1). For the Blodgett site, linear regression analysis carried out for the case 1 showed a better predictive capacity, with a coefficient slope of 0.86 between measured and modeled GPP, when forced to origin (Table 2) than the other two ecosystems, with slopes of 0.74 and 0.77 for Lindcove and Castelporziano sites, respectively. Moreover, when considering the nonlinear nature of the

relationships between GPP and environmental predictors with their combinations (Table S2), the regression slopes between predicted and observed datasets did not improve the predictive capacity of the nonlinear regressive model realized for the case 1. The importance of the predictors assessed by RFA (RF, Fig. 5) confirmed a strong dependence on soil moisture from Castelporziano (29% importance vs. 18% for Blodgett and Lindcove), with a predominant dependence on PAR for the other two ecosystems.

The second case study also included plant transpiration. This increased the predictive capability of the statistical model and showed to be the most important

Table 2 Four case studies were used with a growing number of predictors to predict gross primary productivity (GPP) based on linear model. Predictors in the model (listed in order of importance) are evapotranspiration (ET), photosynthetic active radiation (PAR), soil moisture, vapor pressure deficit (VPD), temperature of the air (Ta), ozone concentration (O₃l), and stomatal ozone deposition (G_{O3}). ns, not significant

Predictors	Blodgett				Lindcove				Castelporziano			
	Beta	Multiple R ²	F	Total	Beta	Multiple R ²	F	Total	Beta	Multiple R ²	F	Total
Case 1												
PAR (μmol m ⁻² s ⁻¹)	-0.722	0.489	46407.180		PAR (μmol m ⁻² s ⁻¹)	0.098	470.028		Soil moisture (%)	-0.414	0.115	176.796
VPD (kpa)	0.457	0.492	210.360		VPD (kpa)	0.156	299.663		PAR (μmol m ⁻² s ⁻¹)	-0.438	0.209	159.452
Ta (°C)	-0.350	0.499	680.680		Ta (°C)	0.162	29.010		VPD (kpa)	0.089	0.215	10.667
Soil moisture (%)	0.087	0.502	320.310		Soil moisture (%)	0.163	6.161		Ta (°C)	0.081	0.217	3.257
R ²			0.5					0.17				0.22
Slope			0.86					0.74				0.77
df			48399					4338				1351
F			12198					211				94
Case 2												
ET (mmol m ⁻² s ⁻¹)	-0.469	0.483	27355.570		PAR (μmol m ⁻² s ⁻¹)	0.098	470.028		Soil moisture (%)	-0.331	0.115	176.796
PAR (μmol m ⁻² s ⁻¹)	-0.308	0.542	3771.650		VPD (kpa)	0.156	299.663		ET (mmol m ⁻² s ⁻¹)	-0.239	0.214	169.705
Soil moisture (%)	0.072	0.546	213.980		ET (mmol m ⁻² s ⁻¹)	0.234	440.230		PAR (μmol m ⁻² s ⁻¹)	-0.323	0.233	32.896
VPD (kpa)	0.375	0.547	71.590		Ta (°C)	0.235	5.738		VPD (kpa)	0.126	0.245	21.623
Ta (°C)	-0.352	0.551	312.320		Soil moisture (%)	0.236	5.394		Ta (°C)	0.121	0.249	7.515
R ²			0.55					0.24				0.25
Slope			0.88					0.76				0.78
df			29254					4338				1356
F			7192					267				89.52
Case 3												
ET (mmol m ⁻² s ⁻¹)	-0.469	0.483	27355.570		PAR (μmol m ⁻² s ⁻¹)	0.098	471.990		Soil moisture (%)	-0.331	0.115	176.796
PAR (μmol m ⁻² s ⁻¹)	-0.308	0.542	3771.650		VPD (kpa)	0.156	298.684		ET (mmol m ⁻² s ⁻¹)	-0.239	0.214	169.705
Soil moisture (%)	0.072	0.546	213.980		ET (mmol m ⁻² s ⁻¹)	0.234	441.996		PAR (μmol m ⁻² s ⁻¹)	-0.323	0.233	32.896

Table 2 (continued)

Predictors	Blodgett				Lindcove				Castelporziano			
	Beta	Multiple R ²	F	Total	Beta	Multiple R ²	F	Total	Beta	Multiple R ²	F	Total
VPD (kpa)	0.375	0.547	71.590		[O ₃] (ppb)	0.106	0.237	14.196	VPD(kpa)	0.126	0.245	21.623
Ta (°C)	-0.352	0.551	312.320		Ta (°C)	0.103	0.238	4.598	Ta (°C)	0.121	0.249	7.515
[O ₃] (ppb)	ns	ns	ns		Soil moisture (%)	0.026002	0.238265	3.5346	[O ₃] (ppb)	ns	ns	ns
R ²				0.55				0.24				0.25
Slope				0.88				0.76				0.78
df				29254				4332				1350
F				7192				225.84				90
Case 4												
ET (mmol m ⁻² s ⁻¹)	-0.730	0.473	21686.430		G _{O3} (m s ⁻¹)	0.053	0.085	272.181	G _{O3} (m s ⁻¹)	-0.347	0.240	422.360
G _{O3} (m s ⁻¹)	0.271	0.525	2639.770		PAR (μmol m ⁻² s ⁻¹)	-0.203	0.152	235.276	Soil moisture (%)	-0.258	0.293	100.616
PAR (μmol m ⁻² s ⁻¹)	-0.242	0.540	813.270		VPD (kpa)	0.385	0.180	99.428	PAR (μmol m ⁻² s ⁻¹)	-0.199	0.308	28.848
VPD (kpa)	0.252	0.548	446.420		ET (mmol m ⁻² s ⁻¹)	-0.461	0.225	168.336	Ta (°C)	0.134	0.314	10.790
Soil moisture (%)	0.062	0.551	131.650		Ta (°C)	0.048	0.226	6.805	ET (mmol m ⁻² s ⁻¹)	-0.056	0.315	2.796
Ta (°C)	-0.082	0.551065	12.11		Soil moisture (%)	0.143966	0.227684	4.8459	VPD (kpa)	ns	ns	ns
R ²				0.55				0.23				0.315
Slope				0.89				0.79				0.79
df				24184				2937				1332
F				4947				144				153

predictor in the Blodgett ecosystem (Table 2), although it was ranked second in importance by the RF (Fig. 5). Notably, even in this second case, the predictor with greater importance in Castelporziano was the soil moisture (Fig. 5), as also highlighted in the linear regression analysis (Table 2). However, soil moisture was not significant *per se* in the nonlinear regression analysis, but only when it was combined with other predictors such as transpiration and PAR (Table S2).

The third case study included $[O_3]$. This predictor did not linearly affect GPP, except in Lindcove (Table 2), where it was ranked 4th in importance. The likelihood of the regression between measured and modeled GPP values by GRMs when the values were forced to origin was high for the Blodgett forest ($R^2 = 0.88$), whereas slopes reached the values of 0.76 and 0.78 for Lindcove and Castelporziano, respectively (Table 2). Same results were observed in nonlinear regression analysis (Table S2).

Case 4 included G_{O_3} , a predictor that showed high statistical significance in all ecosystems under investigation (Table 2) ranking first in Lindcove and Castelporziano (R^2 increase by 0.085 and 0.24 for a summed $R^2 = 0.23$ and 0.31, respectively) and second in Blodgett (R^2 increase by 0.052 for a summed $R^2 = 0.55$). Combinations between G_{O_3} and environmental predictors were not significant as highlighted in the nonlinear regression analysis (Table S2).

The RF is in a good agreement with the statistical analyses except for Blodgett, where PAR still was the predictor with the highest importance. For Blodgett and Lindcove, the importance of G_{O_3} was about 12% and 19%, respectively.

Study of interactions using Granger causality

The spectral extension of G-causality allowed investigating the interactions of GPP and ozone at specific time frequencies. Because of the strong periodic nature of the data at daily cycle demonstrated by the wavelet coherence analysis (Fig. 1–3), we used the spectral extension of G-causality focusing on the daily period and correspondent subharmonic. The time step and length of the data permitted to perform the G-causality analysis at such frequencies with good statistical representation, even for Castelporziano, when less than 1 year of data was available.

Because of the temporal sequence (Eqn 3S), it is clear that G-causality can only capture functional relationships for which cause and effect are sufficiently separated in time. For this reason, we excluded from this analysis PAR and ET, which have strong in-phase correlation with GPP, and soil moisture, because it has no effects at daily scale. The conditional spectral G-causality of G_{O_3} on GPP, given the effects of temperature, VPD, and $[O_3]$ is shown in Fig. 6. Table 3 summarizes the G-causality on GPP, averaged across frequencies between 0.5 and 2.5 day^{-1} considering that most of the G-causality is expressed in this time range (Fig. 6), for the four considered variables, Ta, VPD, $[O_3]$, and G_{O_3} . Table 3 shows that the strongest influence was found for Castelporziano and Lindcove, but significant interactions were also present at Blodgett. For Lindcove and Castelporziano, G_{O_3} was the variable with most predicting power on GPP, but Ta was also very important and the first driver for Blodgett. $[O_3]$ and VPD only showed marginal or no significance for all sites.

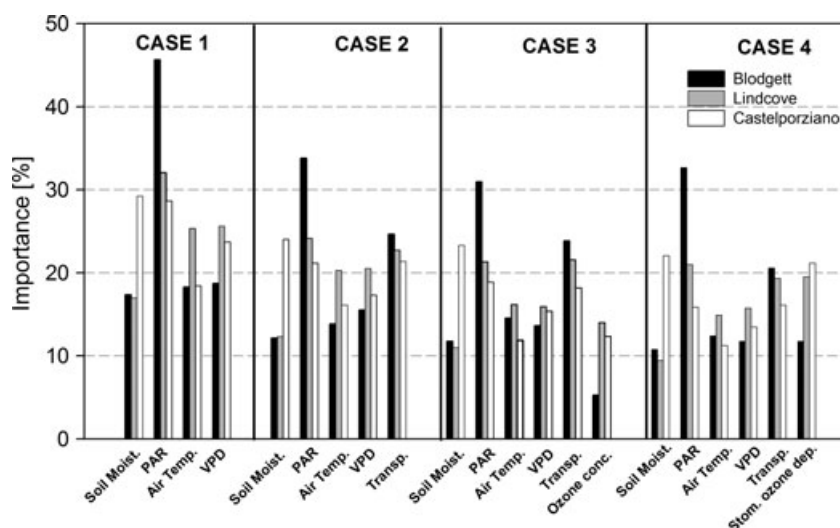


Fig. 5 For each of the four cases investigated, percent importance resulting from the tree analysis of the Random Forest technique is shown. Different colors are to distinguish between the three experimental sites.

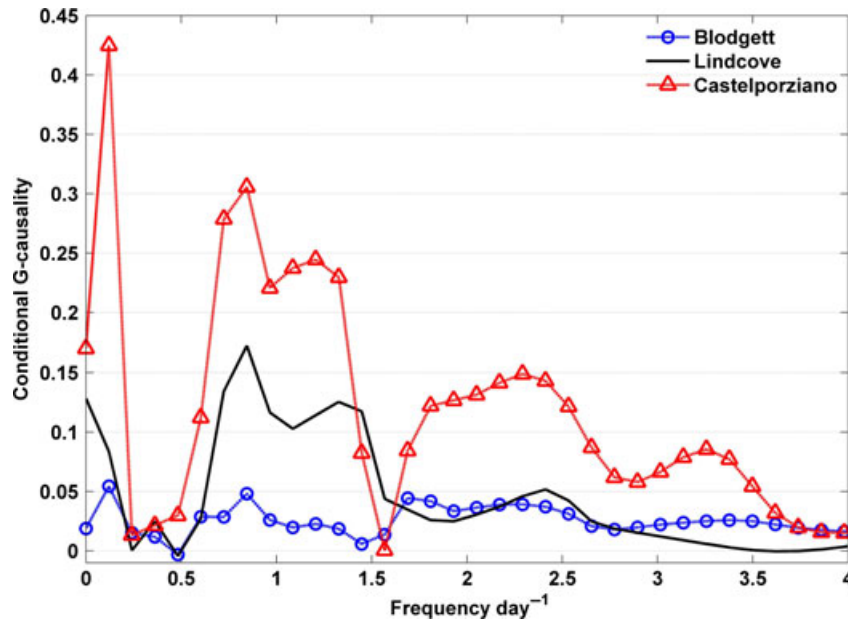


Fig. 6 Conditional G-causality for the influence of G_{O_3} on gross primary productivity (GPP) as function of frequency. The conditional statistic is estimated for a multivariate system, which includes the effects of temperature, vapor pressure deficit (VPD), and $[O_3]$.

Table 3 Conditional G-causality averaged in the frequencies 0.5–2.5 day^{-1} , for the influence of air temperature (Ta), VPD, O_3 concentration ($[O_3]$), and stomatal O_3 deposition ($[G_{O_3}]$) on gross primary productivity (GPP). ns, not significant

Blodgett Predictors	G-causality	Lindcove Predictors	G-causality	Castelporziano Predictors	G-causality
Ta	0.0399	G_{O_3}	0.0753	G_{O_3}	0.1631
G_{O_3}	0.0302	Ta	0.0668	Ta	0.1374
$[O_3]$	0.0107	VPD	0.0134	VPD	0.0151
VPD	ns	$[O_3]$	0.0117	$[O_3]$	0.0027

Discussion

The availability of continuous measurements of atmospheric ozone concentration and eco-physiological parameters demonstrated the detrimental effect of ozone on GPP at two forest ecosystems and an orange orchard. Our results support the hypothesis that G_{O_3} performed better than $[O_3]$ in predicting a reduction in carbon assimilation. The larger implication of these results is that global carbon models may overestimate GPP if the negative effect of ozone is not taken into account. Here, we discuss the interpretation and implications for each analysis in our experiment.

Study of temporal correlations using wavelet coherence analysis

Overall, our results showed high temporal correlation between GPP and G_{O_3} associated with low values of GPP and higher $[O_3]$ at all study sites (Fig. 1–3; Fig. S1).

We tested the hypothesis that, once the confounding effects of PAR and Ta on GPP have been removed, the reduction in GPP is likely driven by elevated atmospheric-level $[O_3]$ or ozone entering through stomata. Our results showed that this temporal correlation is not constant through time due to the effects of seasonal (e.g., cold periods) and sporadic (e.g., precipitation) climate conditions on plant physiology. Similar to our study, inconsistencies of the relationships between other biometeorological variables and GPP have been observed in other forest ecosystems (Vargas *et al.*, 2011). These results open research opportunities to further explore the multitemporal and multifactor variables that control biometeorological responses across the soil–plant–atmosphere continuum.

A major point of discussion is whether within-season responses prevail over carry-over effects in the following year (Hayes *et al.*, 2011). Carry-over effects usually occur as reduced growth of shoots and roots following ozone exposure (Oksanen & Saleem, 1999; Yonekura

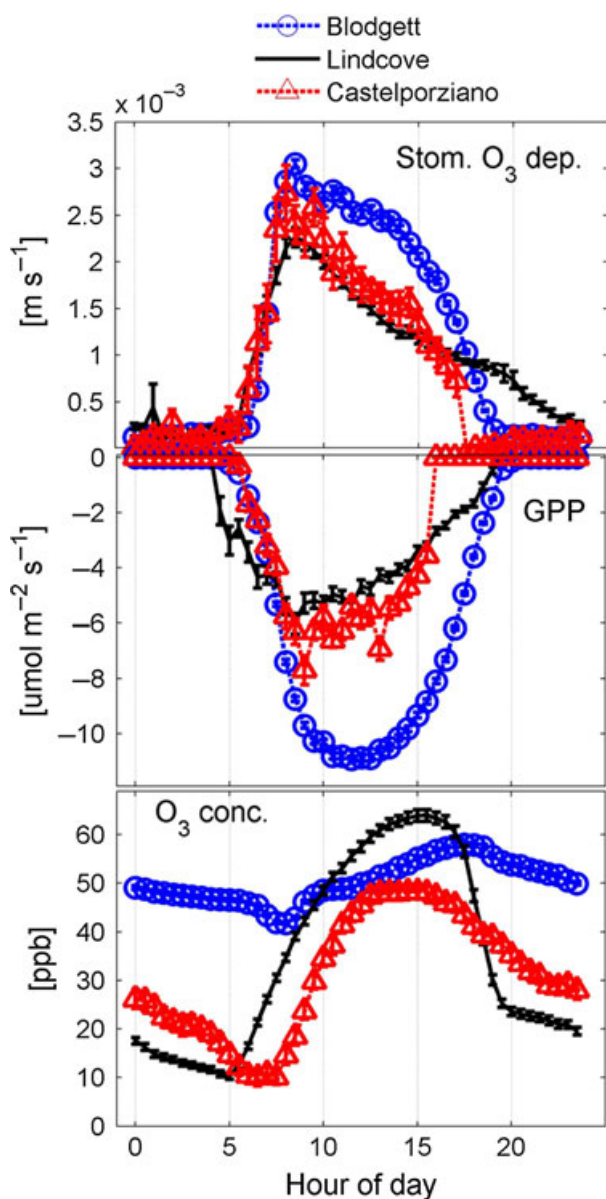


Fig. 7 Hourly values of G_{O_3} , gross primary productivity (GPP), and $[O_3]$ measured in the three ecosystems under investigation in this study. Data are filtered for the day of the year 60–263 for Blodgett and Lindcove, whereas for Castelporziano, we used the day of the year 249–293. Error bars indicate SD.

et al., 2004; Riikonen *et al.*, 2008). Our multiyear analysis on Blodgett showed the highest correlations at 1 d scale, although we cannot exclude additive effects over the years, looking at the correlations at 64–128 d scales. Similar results were observed for Lindcove and Castelporziano, where high correlations were associated with low GPP values and high levels of $[O_3]$. Furthermore, at all sites, the slopes of G_{O_3} with GPP decreased at increasing $[O_3]$, supporting our hypothesis and previous experimental observations that an

increase in $[O_3]$ and deposition through stomata could decrease carbon assimilation (Lombardozzi *et al.*, 2012). Previous research (McLaughlin *et al.*, 2007) showed increased water losses from a mixed deciduous forest in response to high $[O_3]$. The authors reported an increased sap flow due to an amplification of diurnal patterns of water losses. Sluggish stomatal responses to fluctuating stimuli are induced by ozone exposure and can justify such increased water losses (Paoletti & Grulke, 2010). Although we cannot demonstrate this phenomenon in our field sites, we postulate that this compromised water-use control could be a reason for decoupling between GPP and G_{O_3} in conditions of high levels of $[O_3]$.

Significant temporal correlations were also observed at higher frequencies (64 d) for the Blodgett site in correspondence of summer period, except for the years 2001 and 2002, when correlation was good through all the year. Our data show that during warm seasons, atmospheric ozone concentrations are high and GPP is maximized, thus suggesting that the highest correlations between GPP and G_{O_3} or $[O_3]$ occur during this physiologically active period. This is in agreement with the findings from Fares *et al.* (2010b), which showed that this pine forest is a high ozone sink especially in the spring–summer seasons. For Blodgett, precipitation was scarce (36 mm in August; Table 1), but enough to maintain humidity in soils (volumetric water content near 10%) during summer months (Table 1), and mean temperatures and VPD calculated for the day hours did not represent limiting conditions for carbon assimilation (NEE about $-200 \text{ g C m}^{-2} \text{ month}^{-1}$). Therefore, higher carbon assimilation could potentially sustain the negative effects of higher ozone concentrations in this growing forest site and explain those observations (ca. 18% of days) of lower consistency of the temporal correlation between G_{O_3} and GPP at the 1 day period.

In contrast to Blodgett and Castelporziano, the Lindcove site did not experience water scarcity as it was irrigated all year round (volumetric water content above 20%), but experienced high values of ozone concentration and VPD (up to 72 ppb and 3.73 kPa in July, respectively). Such conditions, together with phenological modifications (flowering), are likely a reason for low levels of carbon assimilation. Therefore, the Citrus ecosystem was a carbon source in summer months (NEE 89 g C m^{-2} in July), but harvesting and pruning during the late spring removed a considerable amount of biomass and photosynthesis surface. Our results showed that significant temporal correlations at the 1 day period between G_{O_3} and GPP were common between May and August (DOY 170–240). These dates represented the hottest months, where ozone is high and VPD is a limiting condition for photosynthesis,

likely responsible for a decrease in GPP (Fig. 2e). The high consistency (ca. 48% of days) of the temporal correlation between G_{O_3} and GPP at the 1 day period suggests that this managed plantation could be more susceptible to high ozone concentration, also considering that this orchard was showed as an active ozone sink in the warm seasons (Fares *et al.*, 2012). In contrast to Blodgett and Castelporziano, the Lindcove site showed the correlation at the 1 day with a 2 h lag, with G_{O_3} rising before GPP. This mismatch between stomatal aperture and GPP may provide insights that oxidative processes take place after ozone entry through stomata, as also observed by previous research (Wohlgemuth *et al.*, 2002; Paoletti & Grulke, 2005; Castagna & Ranieri, 2009). However, we cannot explain why this hypothesized oxidative burst was not observed in the forest sites. It may be possible that this delayed relationship does not necessarily have to be interpreted as a damage to plant, but in a wider ecological sense as a different physiological adaptation of plants in response to ozone variability. There are limited evidences in literature that describe high sensitivity to ozone for orange trees (Olszyk *et al.*, 1992). However, the Lindcove site experienced the highest ozone levels among the three sites (Table 1). It is therefore plausible that in the California central valley, ozone reached the highest levels of toxicity in comparison with the other two sites.

Statistical models to highlight dependence of GPP on ozone

To quantify this effect of increasing $[O_3]$ on GPP, we performed a detailed statistical analysis to take into account each single effect on GPP for all predictors and their combinations. For all case studies, linear correlation analysis showed a better predictive capacity for the Blodgett site (i.e., higher coefficient slopes between measured and modeled GPP; Table 2). However, the likelihood of the regression between measured and modeled GPP values is dependent on the testing dataset, and demonstrates the importance of a rich dataset for interpretation of environmental effects on GPP.

In case study 1, PAR was the predictor that better explained GPP for Blodgett and Lindcove (Table 2), followed by VPD, air temperature, and soil moisture, whereas ET became the most significant predictor in case study 2 for Blodgett. In Castelporziano, soil moisture was the most significant predictor, even when ET was included in the analysis. The RF confirmed the dependence on soil moisture from Castelporziano (29% importance vs. 18% for Blodgett and Lindcove for case 1), whereas in the nonlinear regression analysis, soil moisture was important in combination with other predictors such as transpiration and PAR (Table 3). We

explain the sensitivity to soil moisture from Castelporziano with its lower soil moisture in comparison with the other ecosystems (Table 1). Averaged in the years 2007–2011, annual precipitation in Castelporziano was 805 ± 256 mm, but concentrated in the winter months. Moreover, the soil has a sandy texture and low water-holding capacity, which exacerbates early drought (more details in Fares *et al.*, 2009). This supports the hypothesis that the first two ecosystems are less dependent on soil water content because water availability was not a severe limiting factor, as discussed earlier in the text. However, if soil moisture was not the main limiting factor for Blodgett and Lindcove sites, VPD had a negative effect on GPP, as shown in Table 2 and reported in Fares *et al.* (2012).

The third case study included $[O_3]$, under the assumption that a correlation exists between exposure to the pollutant and reduction in carbon assimilation. This correlation has been proved by controlled experiments in which plants were exposed to known concentration of the pollutant, and ozone-exposure metrics for risk assessment were developed (e.g., AOT40, SUM0) for a large category of crop and forest species (Karlsson *et al.*, 2000; Manning, 2005; EPA, 2007; UNECE, 2011). In our study, $[O_3]$ did not have any significant effect in terms of increased R^2 or slopes except for Lindcove (Table 2), both using linear and nonlinear models. These results stress the concept that if ozone damage exists, a flux-based metric may be more appropriate at least for Mediterranean ecosystems, where there is an evident mismatch between the hour of the day when stomatal conductance reaches the maximum (morning) and the hour of the day when ozone concentration peaks with the typical bell-shaped dynamics (noon to 02:00 hours, Fig. 7) as reported previously (Matussek *et al.*, 2007; Fares *et al.*, 2010a, b). In Lindcove, the negative effect of ozone can be explained by the very high levels of ozone fluxes through the stomata, due to the high concentrations of tropospheric ozone typical of the Central Valley of California, often exceeding 60 ppb as an hourly average for the growing season (Table 1; Fig. 2), with peaks above 100 ppb during the warm months of June and August (Fares *et al.*, 2012). Moreover, in this orchard, the intense irrigation tends to make stomata more open during the central hours of the day (Fig. 7), although a VPD limiting effect has been shown (Fares *et al.*, 2012).

With the inclusion of G_{O_3} in case 4, the higher statistical significance was reached for all ecosystems under investigation (Table 2). Similar results were reported by Zapletal *et al.* (2011), where the highest percentage of explained variability in the NEP of a Norway spruce (*Picea abies*) forest was obtained using stomatal ozone flux rather than $[O_3]$. This case study also revealed that

in Blodgett and Lindcove, the predictor assumes positive sign similar to $[O_3]$ (Table 2), thus suggesting that a negative effect of ozone occurs in Blodgett and Lindcove. Under the assumption that those coefficients can be considered as quantification of GPP reduction, results from the RF evaluation offer a quantification of ozone damage equal to 12% and 19% for Blodgett and Lindcove, respectively. Results suggest that ozone impacts on GPP cannot be neglected in Mediterranean forest ecosystems where ozone concentrations are high and drought does not represent a severe limiting factor. In agreement with our findings, a study from De Marco *et al.* (2010) showed that the yield variability explained by important environmental factors such as soil water content, air temperature, light, and relative humidity was lower than the variability explained by G_{O_3} for durum wheat (*Triticum durum*) in central Italy. In Castelporziano, the sign of G_{O_3} is negative (Table 2), thus excluding that this predictor can be an indicator of ozone damage to GPP over the autumnal period of investigation (September–December). Especially in the warmer month of September, ozone concentration in Castelporziano was much lower in comparison with the other two ecosystems (Table 1), and cumulated stomatal ozone fluxes were also lower, with values of $0.03 \text{ g O}_3 \text{ m}^{-2}$ vs. 0.09 and $0.17 \text{ g O}_3 \text{ m}^{-2}$ measured in Blodgett and Lindcove, respectively (Table 1, Fig. 7). This minor phytotoxic ozone dose, which reached the intercellular spaces of leaves (Fares *et al.*, 2013), may suggest that ozone did not represent a limiting factor for the tree species in Castelporziano. Moreover, although *P. ponderosa* grown in the California Sierra Mountains and *Citrus* are considered to be sensitive species to ozone exposure (Olszyk *et al.*, 1992; Arbaugh *et al.*, 1998), the sclerophyll Oak species (*Q. suber*, *Q. ilex*) and Stone Pines (*P. pinea*) occurring in the footprint area of the measuring site of Castelporziano have been previously characterized by operating a water saving strategy, with midday stomatal closure under moderate heat and drought stress, and thick cuticles to contain water losses, which likely provide resistance to ozone (Manes *et al.*, 1997, 2006; Fares *et al.*, 2009; Mereu *et al.*, 2009). The finding that, differently from Blodgett and Lindcove, the ecosystem in Castelporziano was a carbon source rather than a carbon sink during the measurement period (positive values of NEE, Table 1) is another indicator that species-specific differences may be the basis of a higher resistance to ozone of Castelporziano tree species.

Study of interactions using Granger causality

This method expresses linear directional coupling among variables of complex systems, and differs from

the previous statistical approach because a significant effect of a variable over GPP is based on the improved ability to forecast GPP once past states of that variable are taken into account. G-causality provided an additional quantification of the magnitude and direction of interactions between variables at a specific frequency, but not the sign. However, this represents an independent method to verify if the absolute amount of the interaction is in agreement with the other methods. In Castelporziano and Lindcove, we found the strongest interactions between G_{O_3} and GPP, but significant interactions were also observed at Blodgett, ranked second after ambient temperature (Fig. 6; Table 3). In agreement with our previous analyses, $[O_3]$ and VPD showed only limited or nonsignificant effects. This result also supports the hypothesis that G_{O_3} interacts with GPP influencing future response of plant to assimilate carbon, even when the effects of potential confounding variables are taken into account.

In conclusion, our results derived from three independent methodologies suggest that rising ozone pollution, an often overlooked aspect of global atmospheric change, reduced the ability of Mediterranean plant ecosystems to assimilate carbon. We found that the negative effects of ozone on GPP mainly occurred within a day of exposure/uptake. We found that as ozone concentrations rise, any increase in stomatal aperture became less strongly linked with GPP increase. These results imply that ozone uptake has a direct negative effect on carbon assimilation by plants. Up to 12–19% of the carbon assimilation reduction in *P. ponderosa* and in *C. sinensis* was explained by stomatal ozone deposition. We did not observe limiting effect on GPP in the mixed Oak ecosystem probably due to higher stomatal resistance of the sclerophyll species and the exposure to lower ozone concentration. However, 4 months of measurements may have not been enough to untangle a negative effect of ozone from the effects of confounding factors, thus supporting the importance of using continuous long-term measurements of ecophysiological parameters to explain ozone damage to real-world forests. We emphasize that ozone exposure is not a reliable indicator for ozone-risk assessment in Mediterranean ecosystems and urge that flux-based approach be used instead.

Acknowledgements

The research in Blodgett was made possible by grants from the Kearney Foundation of Soil Science, the University of California Agricultural Experiment Station and the Office of Science, Biological and Environmental Research Program (BER), U.S. Department of Energy, through the Western Regional Center of the National Institute for Global Environmental Change (NIGEC) under Cooperative Agreement No. DEFCO2-03ER63613. We

gratefully acknowledge Dr. Megan McKay for helping to collect the data.

The research in Lindcove was made possible by grants from the Citrus Research Board, the California Air Resources Board, and by the European Commission Marie Curie IOF 2008 project CITROVOC. We gratefully acknowledge Dr. Robin Weber for helping to collect the data.

The research in Castelporziano was supported by the LIFE10 ENV/FR/2008 project FO₃REST, by the UE Marie Curie project EXPL03RVOOC, by projects 'CASTELTOF' and 'CASTEL2' financed by the General Secretariat of the Presidency of Italian Republic. We gratefully acknowledge the Multi-disciplinary Center for the Study of Coastal Mediterranean Ecosystems, in particular Ing. Alejandro Tinelli and Dr. Luca Maffei, for technical and logistic support allowing execution of these studies and publication of the data; and the team members of the biometeorology laboratory at CRA: Mr. Valerio Moretti, Mr. Tiziano Sorgi and Mr. Filippo Ilardi, for their help with setting up the experimental station. Dr. Francesco Loreto and Prof. Giuseppe Scarascia Mugnozza are acknowledged for their scientific collaboration within the above-mentioned projects.

References

- Arbaugh MJ, Miller PR, Caroll JJ, Takemoto B, Proctor T (1998) Relationships of ozone exposure to pine injury in the Sierra Nevada and San Bernardino mountains of California, USA. *Environmental Pollution*, **101**, 291–301.
- Blanken PD, Black TA, Yang PC *et al.* (1997) Energy balance and canopy conductance of a boreal aspen forest: partitioning overstory and understory components. *Journal of Geophysical Research*, **102**, 915–927.
- Breiman L (2001) Random forests. *Machine Learning*, **45**, 5–32.
- Breiman L, Friedman JH, Olshen RA, Stone CJ (1984) *Classification and Regression Trees*. Wadsworth & Brooks/Cole Advanced Books & Software, Monterey, CA.
- Castagna A, Ranieri A (2009) Detoxification and repair process of ozone injury: from O₃ uptake to gene expression adjustment. *Environmental Pollution*, **157**, 1461–1469.
- Chameides WL, Lindsay RW, Richardson J, Kiang CS (1988) The role of biogenic hydrocarbons in urban photochemical smog: Atlanta as a case study. *Science*, **241**, 1473–1475.
- Cooper OR, Parrish DD, Stohl A *et al.* (2010) Increasing springtime ozone mixing ratios in the free troposphere over western North America. *Nature*, **463**, 344–348.
- De Marco A, Screpanti A, Paoletti E (2010) Geostatistics as a validation tool for setting ozone standards for durum wheat. *Environmental Pollution*, **158**, 536–542.
- Detto M, Baldocchi D, Katul G (2010) Scaling properties of biologically active scalar concentration fluctuations in the surface layer over a managed peatland. *Boundary Layer Meteorology*, **136**, 407–430.
- Detto M, Molini A, Katul G, Stoy P, Palmroth S, Baldocchi D (2012) Causality and persistence in ecological systems: a nonparametric spectral Granger causality approach. *American Naturalist*, **179**, 524–535.
- Emberson LD, Wieser G, Ashmore MR (2000) Modelling of stomatal conductance and ozone flux of Norway spruce: comparison with field data. *Environmental Pollution*, **109**, 393–402.
- EPA (2007) *Review of the National Ambient Air Quality Standards for Ozone: Policy Assessment of Scientific and Technical Information*. OAQPS Staff Paper. U.S. Environmental Protection Agency, Office of Air Quality Planning and Standards, Research Triangle Park, Durham NC. Publication No. EPA-452/R-07-003.
- Fares S, Mereu S, Scarascia Mugnozza G *et al.* (2009) The ACCENT-VOCBAS field campaign on biosphere-atmosphere interactions in a Mediterranean ecosystem of Castelporziano (Rome): site characteristics, climatic and meteorological conditions, and eco-physiology of vegetation. *Biogeosciences*, **6**, 1043–1058.
- Fares S, McKay M, Holzinger R, Goldstein AH (2010a) Ozone fluxes in a *Pinus ponderosa* ecosystem are dominated by non-stomatal processes: evidence from long-term continuous measurements. *Agricultural and Forest Meteorology*, **150**, 420–431.
- Fares S, Goldstein A, Loreto F (2010b) Determinants of ozone fluxes and metrics for ozone risk assessment in plants. *Journal of Experimental Botany*, **61**, 629–633.
- Fares S, Weber R, Park J-H, Gentner D, Karlik J, Goldstein AH (2012) Ozone deposition to an orange orchard: partitioning between stomatal and non-stomatal sinks. *Environmental Pollution*, **169**, 258–266.
- Fares S, Matteucci G, Scarascia Mugnozza G *et al.* (2013) Testing of models of stomatal ozone fluxes with field measurements in a mixed Mediterranean forest. *Atmospheric Environment*, **67**, 242–251.
- Fowler D, Pilegaard K, Sutton M *et al.* (2009) Atmospheric composition change: ecosystems-atmosphere interactions. *Atmospheric Environment*, **43**, 5193–5267.
- Geider RJ, Delucia EH, Falkowski PG *et al.* (2001) Primary productivity of planet Earth: biological determinants and physical constraints in terrestrial and aquatic habitats. *Global Change Biology*, **7**, 849–882.
- Goldstein AH, Hultman NE, Fracheboud JM *et al.* (2000) Effects of climate variability on the carbon dioxide, water, and sensible heat fluxes above a ponderosa pine plantation in the Sierra Nevada (CA). *Agricultural and Forest Meteorology*, **101**, 113–129.
- Grace J (2004) Understanding and managing the global carbon cycle. *Journal of Ecology*, **92**, 189–202.
- Granger CWJ (1969) Investigating causal relations by econometric models and cross-spectral methods. *Econometrica*, **37**, 424–438.
- Grunsted A, Moore JC, Jevrejeva S (2004) Application of the cross wavelet transform and wavelet coherence to geophysical time series. *Nonlinear Processes in Geophysics*, **11**, 561–566.
- Hayes F, Mills G, Harmens H, Wyness K (2011) Within season and carry-over effects following exposure of grassland species mixtures to increasing background ozone. *Environmental Pollution*, **159**, 2420–2426.
- Heinemeyer A, Wilkinson M, Vargas R, Subke JA, Casella E, Morison JIL, Ineson P (2012) Exploring the “overflow tap” theory: linking forest soil CO₂ fluxes and individual mycorrhizosphere components to photosynthesis. *Biogeosciences*, **9**, 79–95.
- Karlsson PE, Pleijel H, Pihl Karlsson G, Medin EL, Skärby L (2000) Simulations of stomatal conductance and ozone uptake to Norway spruce saplings in open-top chambers. *Environmental Pollution*, **109**, 443–451.
- Katul G, Lai CT, Schafer K, Vidakovic B, Albertson J, Ellsworth D, Oren R (2001) Multiscale analysis of vegetation surface fluxes: from seconds to years. *Advances in Water Resources*, **24**, 1119–1132.
- Lasslop G, Reichstein M, Papale D *et al.* (2010) Separation of net ecosystem exchange into assimilation and respiration using a light response curve approach: critical issues and global evaluation. *Global Change Biology*, **16**, 187–208.
- Lombardozzi D, Levis S, Bonan G, Sparks JP (2012) Predicting photosynthesis and transpiration responses to ozone: decoupling modeled photosynthesis and stomatal conductance. *Biogeosciences*, **9**, 3113–3313.
- Manes F, Seufert G, Vitale M (1997) Ecophysiological studies of Mediterranean plant species at the Castelporziano estate. *Atmospheric Environment*, **31**, 51–60.
- Manes F, Vitale M, Donato E, Giannini M, Puppi G (2006) Different ability of three Mediterranean oak species to tolerate progressive dehydration stress. *Photosynthetica*, **44**, 387–393.
- Manes F, Vitale M, Fabi MA, De Santis F, Zona D (2007) Estimates of potential ozone stomatal uptake in mature trees of *Quercus ilex* in a Mediterranean climate. *Environmental and Experimental Botany*, **59**, 235–241.
- Manning WJ (2005) Establishing a cause and effect relationship for ambient ozone exposure and tree growth in the forest: progress and an experimental approach. *Environmental Pollution*, **137**, 443–454.
- Matyssek R, Bytnerowicz A, Karlsson PE, Paoletti E, Sanz M, Schaub M, Wieser G (2007) Promoting the O₃ flux concept for European forest trees. *Environmental Pollution*, **146**, 587–607.
- McLaughlin SB, Nosal M, Wullschlegel SD, Sun G (2007) Interactive effects of ozone and climate on tree growth and water use in a southern Appalachian forest in the USA. *New Phytologist*, **174**, 109–124.
- Mereu S, Salvatori E, Fusaro L, Gerosa G, Muys B, Manes F, Leuven KU (2009) An integrated approach shows different use of water resources from Mediterranean maquis species in a coastal dune ecosystem. *Biogeosciences*, **6**, 2599–2610.
- Mills G, Pleijel H, Braun S *et al.* (2011) New stomatal flux-based critical levels for ozone effects on vegetation. *Atmospheric Environment*, **45**, 5064–5068.
- Oksanen E, Saleem A (1999) Ozone exposure results in various carry-over effects and prolonged reduction in biomass in birch (*Betula pendula* Roth). *Plant, Cell and Environment*, **22**, 1401–1411.
- Olszyk DM, Takemoto BK, Kats G, Dawson PJ, Morrison CL, Wolf Preston J, Thompson CR (1992) Effects of open-top chambers on ‘Valencia’ orange trees. *Journal of Environmental Quality*, **21**, 128–134.
- Paoletti E (2006) Impact of ozone on Mediterranean forests: a review. *Environmental Pollution*, **144**, 463–474.
- Paoletti E, Grulke NE (2005) Does living in elevated CO₂ ameliorate tree response to ozone? A review on stomatal responses. *Environmental Pollution*, **137**, 483–493.
- Paoletti E, Grulke NE (2010) Ozone exposure and stomatal sluggishness in different plant physiognomic classes. *Environmental Pollution*, **158**, 2664–2671.

- Paoletti E, Manning WJ (2007) Toward a biologically significant and usable standard for ozone that will also protect plants. *Environmental Pollution*, **150**, 85–95.
- Riikonen J, Kets K, Darbah J *et al.* (2008) Carbon gain and bud physiology in *Populus tremuloides* and *Betula papyrifera* grown under long-term exposure to elevated concentrations of CO₂ and O₃. *Tree Physiology*, **28**, 243–254.
- Samuelson L, Kelly JM (2001) Scaling ozone effects from seedlings to forest trees. *Tansley Review* 21. *New Phytologist*, **149**, 21–41.
- Torrence C, Compo GP (1998) A practical guide to wavelet analysis. *Bulletin of the American Meteorological Society*, **79**, 61–78.
- UNECE (2011) Manual on Methodologies and Criteria for Modelling and Mapping Critical Loads & Levels and Air Pollution Effects, Risks and Trends. Convention on Long-range Transboundary Air Pollution. Available at: <http://www.icpmapping.org> (accessed November 2012).
- Vargas R, Detto M, Baldocchi DD, Allen MF (2010) Multiscale analysis of temporal variability of soil CO₂ production as influenced by weather and vegetation. *Global Change Biology*, **16**, 1589–1605.
- Vargas R, Baldocchi DD, Bahn M *et al.* (2011) On the multi-temporal correlation between photosynthesis and soil CO₂ efflux: reconciling lags and observations. *New Phytologist*, **191**, 1006–1017.
- Vingarzan R (2004) A review of surface ozone background levels and trends. *Atmospheric Environment*, **38**, 3431–3442.
- Wittig VE, Ainsworth E, Long SP (2007) To what extent do current and projected increases in surface ozone affect photosynthesis and stomatal conductance of trees? A meta-analytic review of the last 3 decades of experiments. *Plant, Cell and Environment*, **30**, 1150–1162.
- Wittig VE, Ainsworth E, Naidu SL, Karnosky DF, Long SP (2009) Quantifying the impact of current and future tropospheric ozone on tree biomass, growth, physiology and biochemistry: a quantitative meta-analysis. *Global Change Biology*, **15**, 396–424.
- Wohlgemuth H, Mittelstrass K, Kschieschan S *et al.* (2002) Activation of an oxidative burst is a general feature of sensitive plants exposed to the air pollutant ozone. *Plant, Cell and Environment*, **25**, 717–726.
- Wolfe GM, Thornton JA, McKay M, Goldstein AH (2011) Forest-atmosphere exchange of ozone: sensitivity to very reactive biogenic VOC emissions and implications for in-canopy photochemistry. *Atmospheric Chemistry and Physics*, **11**, 7875–7891.
- Yonekura T, Yoshidome M, Watanabe M, Honda Y, Ogiwara I, Izuta T (2004) Carry-over effects of ozone and water stress on leaf phenological characteristics and bud frost hardiness of *Fagus crenata* seedlings. *Trees*, **18**, 581–588.
- Zapletal M, Cudlín P, Chroust P *et al.* (2011) Ozone flux over a Norway spruce forest and correlation with net ecosystem production. *Environmental Pollution*, **159**, 1024–1034.

Supporting Information

Additional Supporting Information may be found in the online version of this article:

Figure S1. Wavelet coherence analysis to look the temporal correlations between the residuals of gross primary productivity (GPP) and stomatal ozone deposition for the Blodgett site.

Figure S2. For each year in Blodgett site, relationship between the residuals of gross primary productivity (GPP) at the 1 day time period and the residuals of stomatal ozone deposition (G_{O3}) at the 1 day time period for grouped episodes of atmospheric ground-level ozone concentration: low (<50 ppb), medium (>50 and <75 ppb), and high (>75 ppb).

Table S1. Results from regression analysis of residuals of gross primary productivity (residuals GPP) and stomata ozone deposition (residuals G_{O3}) divided by year of measurements in Blodgett (2001–2007) for grouped episodes of atmospheric ozone concentrations.

Table S2. Predictor's coefficients (beta) from the nonlinear General Regression Model (GRM) model applied to the four case studies in the three ecosystems: Blodgett pine forest, Lindcove orange plantation, and Castelporziano mixed forest